LA-UR-09-01120

Title: Measuring Multiple Residual Stress Components using the Contour Method and Multiple Cuts

Author(s):
P. Pagliaro (U. Palermo)
M. B. Prime (W-13)
H. Swenson (MST-6)
B. Zuccarello (U. Palermo)

Details: Experimental Mechanics, 50(2), pp. 187-194, 2010.

Measuring Multiple Residual-Stress Components using the Contour Method and Multiple Cuts

Pierluigi Pagliaro,[1§] Michael B. Prime, [2*] Hunter Swenson, [2] Bernardo Zuccarello[1]

[1] Dipartimento di Meccanica, Universita degli Studi di Palermo, 90128 Palermo, Italy
[2] Los Alamos National Laboratory, Los Alamos, NM 87545 USA
* Corresponding Author, prime@lanl.gov, +1 505 667-1051, Member SEM
[§] Visiting student at Los Alamos National Laboratory

Abstract

The conventional contour method determines one component of residual stress over the cross section of a part. The part is cut into two, the contour (topographic shape) of the exposed surface is measured, and Bueckner's superposition principle is analytically applied to calculate stresses. In this paper, the contour method is extended to the measurement of multiple residual-stress components by making multiple cuts with subsequent applications of superposition. The theory and limitations are described. The theory is experimentally tested on a 316L stainless steel disk with residual stresses induced by plastically indenting the central portion of the disk. The multiple-cut contour method results agree very well with independent measurements using neutron diffraction and with a computational, finite-element model of the indentation process.

Introduction

The recently introduced contour method provides residual-stress measurement capabilities that cannot always be duplicated by other techniques [1], most notably the ability to make a two-dimensional (2D) cross-sectional map of residual stresses. In the contour method, the part is cut into two and the measured contour (topographic shape) of the exposed surface is used to calculate residual stresses. The contour method is useful for studying various manufacturing processes such as laser peening [2-5], friction stir welding [3,4,6] and fusion welding [1,7-11]. Some of the applications are quite unique such as mapping stresses in a railroad rail [12], in the region of an individual laser peening pulse [13], and under an impact crater [14].

The conventional contour method can only measure the stress component normal to the cut plane; however, it is also difficult with other techniques to measure a 2D map of multiple residual-stress components. Sectioning techniques, which require multiple cuts and strain gauges, can in principle determine a three-dimensional (3D) stress map [15,16]. These techniques are time consuming and rarely applied. Spatially refined 2D or 3D neutron diffraction stress maps [17] have practical limits because the required beam time grows exponentially with the dimensionality of mapping. The deep hole method can measure multiple stress components through the thickness of a part but only provides a 1D stress profile [18]. An alternate approach for full-field residual stress determination is to use analytical techniques with physically based assumptions, such as eigenstrain, to expand limited measurements to a more complete stress state [5,16,19-24].

There are several approaches, each with unique capabilities, for augmenting the conventional contour method to measure multiple stress components. The method presented in

this paper uses multiple cuts and reconstructs the original residual stress component normal to each cut. Original residual stresses are those before the first cut, rather than the partially relaxed stresses after the first cut. Multiple cuts are already used to measure multiple stress components with the contour method. However, instead of reconstructing the original stresses the partially-relaxed results are compared to finite-element models that simulate the manufacturing process and also the cuts [25]. The "multiaxial" contour method gives all the stress components by making additional cuts at 45 degrees from the first cut and limiting the application to a continually processed part [26,27]. The surface superposition contour method reconstructs multiple stress components on a single-cut plane without additional cuts, but it requires a surface stress measurement technique in addition to the contour method [28].

This study presents the superposition-based theory for the multiple cuts contour method and the theoretical limitations. It shows experimental application on an indented disk with validation against neutron diffraction measurements. The results are also compared with a computational, finite-element model of the indentation process.

Theory

First cut

Before introducing the new theory for multiple cuts, the principle for a single cut is reviewed [29]. The contour method is based on a variation of Bueckner's superposition principle [30]. Figure 1 shows the traditional contour method in steps **A** through **C**. **A** shows the undisturbed part containing the residual stresses that are to be determined. The part is cut in two on the plane $x = 0$ and deforms as residual stresses are released by the cut. **B** shows half of the part in the post-cut state with partially-relaxed stresses. The surface contour is measured at this point. **C** is an analytical step that starts with a stress-free body and then the surface created by the

cut is forced back to its original flat shape. Assuming elasticity, superimposing the partially relaxed stress state in **B** with the change in stress from **C** gives the original residual stress throughout the part:

$$\sigma^{(A)}(x,y,z) = \sigma^{(B)}(x,y,z) + \sigma^{(C)}(x,y,z) \tag{1}$$

where σ without subscripts refers to the entire stress tensor.

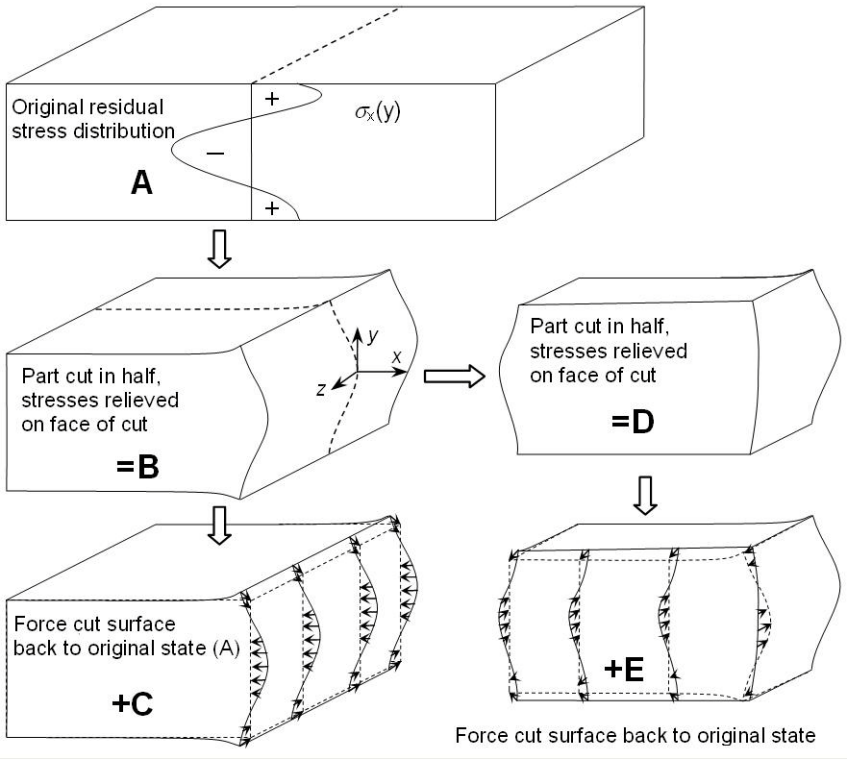

Figure 1. Contour method superposition principle for traditional contour method (A–C) and multiple cuts (D–E). The two cut planes define $x = 0$ and $z = 0$.

Because the partially relaxed stresses in **B** are still unknown, one cannot obtain the original stress throughout the body. However, the normal (σ) and shear (τ) stresses acting on the free surface in **B**, σ_x, τ_{xy} and τ_{xz}, must be zero. Therefore, **C** by itself gives those stresses along the plane of the cut:

$$\begin{aligned} \sigma_x^{(A)}(0,y,z) &= \sigma_x^{(C)}(0,y,z) \\ \tau_{xy}^{(A)}(0,y,z) &= \tau_{xy}^{(C)}(0,y,z) \\ \tau_{xz}^{(A)}(0,y,z) &= \tau_{xz}^{(C)}(0,y,z) \end{aligned} \quad . \tag{2}$$

In practice, only the normal stress component σ_x, can be experimentally determined. The measurement of the contour only provides information about the displacements in the normal direction, not those in the transverse directions. Therefore, the surface is displaced back to the flat configuration in the x-direction only. The shear stresses τ_{xy} and τ_{xz} are constrained to zero in the solution for **C**. This stress-free constraint on the surface is automatically enforced in most structural finite-element analyses if the transverse displacements are left unconstrained.

Multiple cuts

Once the part has been cut in two, the original σ_y or σ_z residual stresses on a different plane can be determined by making an additional cut and applying superposition again. A conventional analysis of data from the second cut provides a map of the stress state after the first cut. Because the first cut causes local relaxation, those are not the original stresses. Fortunately, the same calculation that provides σ_x from the first cut also provides all the necessary information to reconstruct the relevant component of original stresses, for example σ_z, on the plane of the second cut.

For the example of determining σ_z, Figure 1 illustrates the theory for reconstructing the original residual stresses on the plane of the second cut. The part in **B**, which is half of the original part, is cut on the plane $z = 0$. **D** shows the quarter-part deformed by the residual stresses relaxation. **E** is an analytical step in which the surface created by the second cut is forced back to its flat shape before the second cut (**B**). The stress state in **B** is given by superimposing the stress state in **D** with the change in stress from **E**. The original residual stress throughout the part in **A** is therefore given by the sum of the stress states in **D**, **E** and **C**:

$$\begin{aligned}\sigma^{(A)}(x,y,z) &= \sigma^{(B)}(x,y,z) + \sigma^{(C)}(x,y,z) \\ &= \sigma^{(D)}(x,y,z) + \sigma^{(E)}(x,y,z) + \sigma^{(C)}(x,y,z)\end{aligned}. \tag{3}$$

Because the partially relaxed stresses in **D** are unknown, one cannot obtain the original stress throughout the body. However, the normal and shear stresses on the surface in **D**, σ_z, τ_{xz} and τ_{yz}, must be zero. Therefore, the sum of **E**, (equal to **B** on the cut surface) and **C** will give the original stresses along the plane of the second cut:

$$\begin{aligned} \sigma_z^{(A)}(x,y,0) &= \sigma_z^{(E)}(x,y,0) + \sigma_z^{(C)}(x,y,0) \\ \tau_{zx}^{(A)}(x,y,0) &= \tau_{zx}^{(E)}(x,y,0) + \tau_{zx}^{(C)}(x,y,0) \\ \tau_{zy}^{(A)}(x,y,0) &= \tau_{zy}^{(E)}(x,y,0) + \tau_{zy}^{(C)}(x,y,0) \end{aligned} \quad . \tag{4}$$

As before, only the normal stress component σ_z can be experimentally determined.

The same procedure can be applied to obtain the σ_y component if the cut is made along a plane normal to the y-direction instead of the z-direction.

Additional Assumption

An additional assumption, compared to the traditional contour method, is required for accurate results for stresses on the plane of the second or later cuts. One must assume that the shear stresses released by the first cut, $\tau_{xy}^{(A)}(0,y,z)$ and $\tau_{xz}^{(A)}(0,y,z)$, are small. Numerical simulations [28,31] reveal that the limitation is insignificant for most practical applications. The reason for this assumption and an explanation for its minimal effect are given.

The effect of shear stresses can be removed for the traditional single-cut contour method [29]. Normal stresses have a symmetric effect on the two opposing surfaces created by the cut. For example, a tensile stress causes a low spot on both surfaces. Shear stresses, by contrast, have an antisymmetric effect. In the case of symmetric parts, this effect can be averaged away when the contours on both surfaces are measured.

A shear stress effect on multiple cuts does not generally average away. If shear stresses are originally present on the plane of the first cut ($\tau_{xy}^{(A)}(0,y,z)$ and $\tau_{xz}^{(A)}(0,y,z)$), the normal

stresses in **B** will be affected by their relaxation. The perturbation relative to the effect when those shear stresses are zero is antisymmetric with respect to the plane of the cut. So the error on the second cut results can be averaged away only if the original residual stresses are symmetric with respect to the first cut, one makes a third cut symmetric to the second on the opposite half, and all four measured contours are averaged.

The shear stress error is generally small for two reasons: (1) the shear stress magnitudes are usually relatively small, and (2) shear stresses have a reduced effect compared to normal stresses of the same magnitude. Free-boundary conditions require the shear stress components of interest to be zero on much of the boundary of the cut plane. Further, one of the local equilibrium conditions, Eq. 5, limits the rate at which the shear stresses can increase away from the boundary ($\partial\tau_{xy}/\partial y$ and $\partial\tau_{xz}/\partial z$) unless the stress gradient normal to the plane ($\partial\sigma_x/\partial x$) is significant:

$$\frac{\partial\sigma_x}{\partial x}+\frac{\partial\tau_{xy}}{\partial y}+\frac{\partial\tau_{xz}}{\partial z}=0 \quad . \tag{5}$$

The stresses normal to the cut plane have no such boundary restriction, which usually results in higher magnitudes. As for the second reason, the perturbations of the normal stresses in **B** ($\sigma_z^{(B)}(x,y,0)$) are reduced relative to the magnitude of the relaxed shear stress, on the order of the Poisson's ratio. Therefore, assuming the original normal stresses to be measured on the plane of the second cut ($\sigma_z^{(A)}(x,y,0)$) are similar magnitude to those on the first cut ($\sigma_x^{(A)}(0,y,z)$), the shear stress effect on the measured contour and resulting errors are relatively smaller.

Experimental Validation

The theory was experimentally validated on a test specimen with an independently measured residual stress distribution. Indentation can be used to introduce a well-defined residual stress field [32]. For this study, a 60-mm-diameter, 10-mm-thick disk of 316L stainless

steel was plastically compressed on center with opposing 15-mm-diameter hardened steel indenters. The cylindrical indenters were 15 mm in diameter with a 1-mm radius on the edge making for a 13-mm diameter area of initial contact. Complete details were reported previously [33]. The stresses were mapped using neutron diffraction and the single-cut contour method. The indention process was modeled using finite elements (FE) and a quasi-static analysis with a calibrated, cyclic stress-strain model. The two measurement methods agreed with each other and the FE model within 20–30 MPa.

Standard contour method procedure was used to map stresses on two cut planes in the disk. The first cut was a diametrical cut, and a second cut made two quarter sections (refer to Figure 2). The cuts were made using wire electric discharge machining (EDM) with a 100-μm-diameter brass wire. Skim-cut settings were used to minimize introduced stresses. The specimen was securely clamped during cutting to minimize deformation as the stresses relaxed. After cutting, the specimen was removed from the fixture and the contours of the cut surfaces were measured using a laser scanner [34] on a 0.1-mm × 0.04-mm grid.

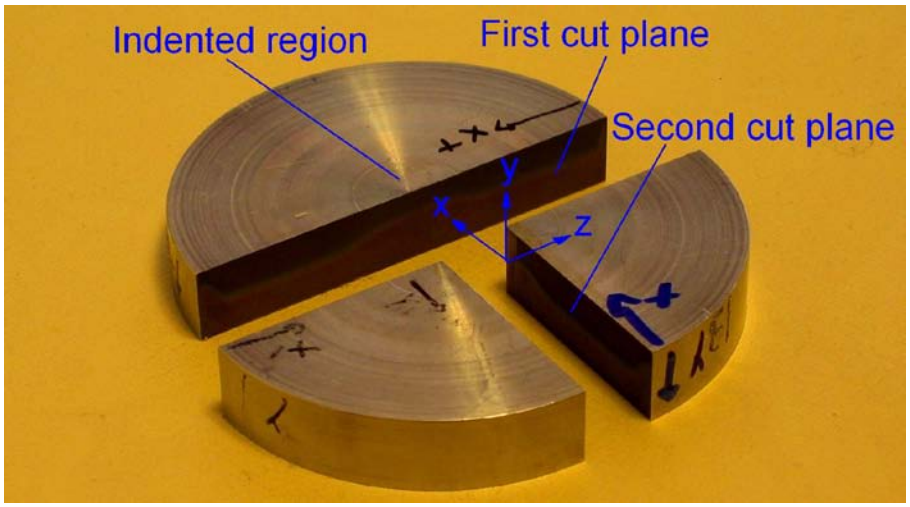

Figure 2. The two cuts used to measure multiple stress components in the steel disk.

The raw data was processed to calculate residual stresses using a standard procedure [34,35]. The point clouds (contour data) from the two opposing surfaces for a given cut were carefully aligned to one another after one cloud was flipped to coincide. The clouds were interpolated onto a common grid and pointwise averaged. Figure 3 shows the averaged contour for the first cut in the disk. Because the discrete data points did not extend all the way to the edges, missing data was filled in by linear extrapolation of interior data [28,35]. The resulting contour was fit to a surface using bivariate splines with the amount of smoothing chosen to minimize uncertainty in the calculated stresses [34]. Figure 4 shows both the measured contour for the second cut and the smoothed spline fit.

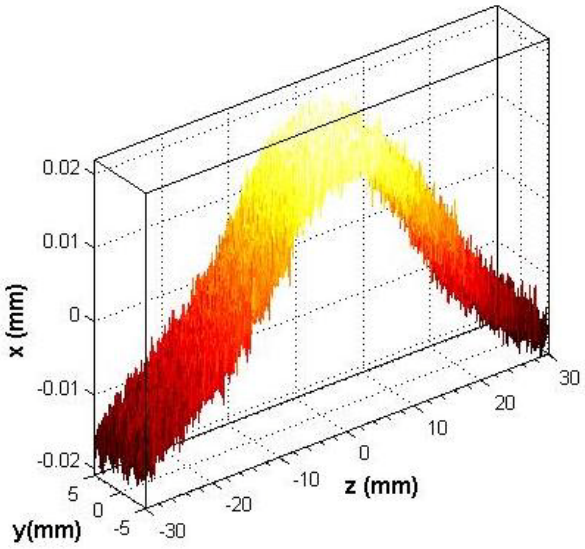

Figure 3. The measured surface contour after the first cut in the disk.

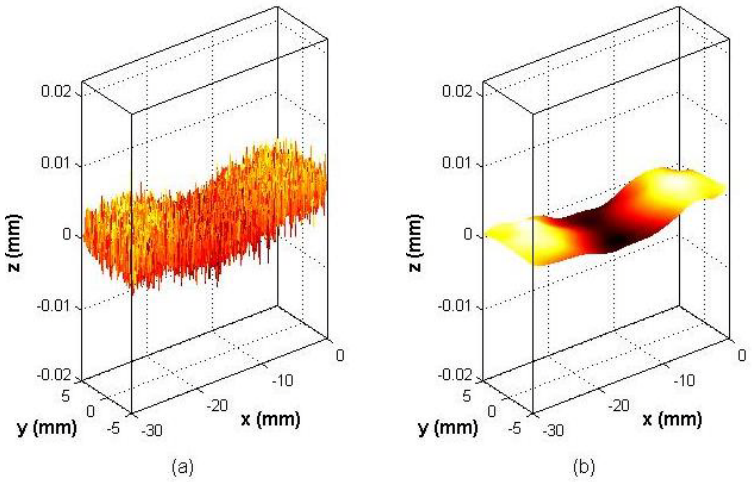

Figure 4. The (a) measured surface contour for the second cut and (b) corresponding smoothed spline fit.

To compute residual stresses, each surface was elastically deformed into the opposite shape of its measured contour (see Figure 5) using a 3D FE model with the Abaqus code [36]. The mesh consisted of linear hexahedral 8-node elements with reduced integration (C3D8R). The material behavior was elastically isotropic with an elastic modulus of 193 GPa and a Poisson's ratio of 0.3. The smoothed surface was evaluated at node locations to write displacement boundary conditions. A static equilibrium step gave the stresses.

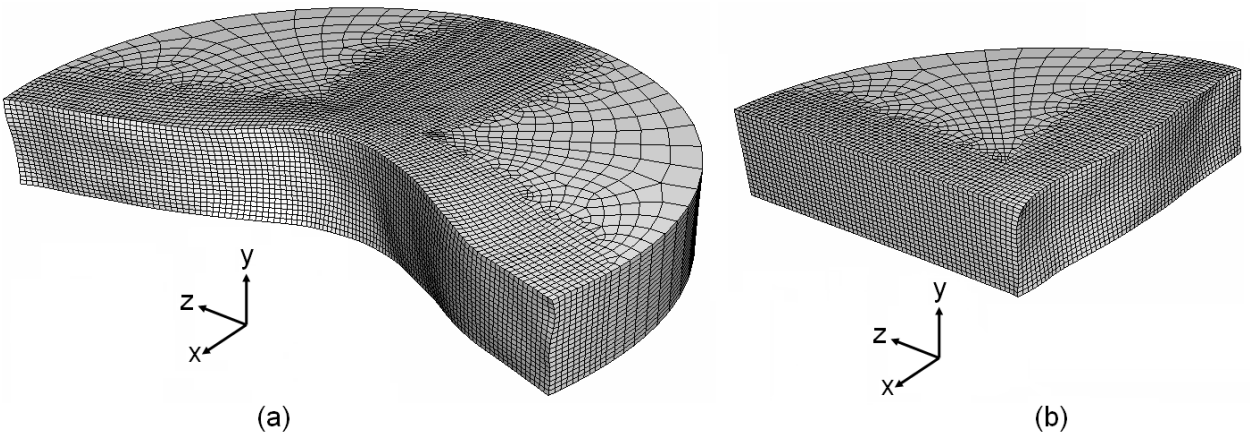

Figure 5. The 3D finite-element model of the disk displaced into the opposite of the measured contour for the (a) first and (b) second cuts.

Finally, the original residual stresses on the plane of the second cut were calculated using superposition from the first line of Eq. 4.

Results

Figure 6 shows the superposition-based reconstruction of the original residual stresses on the plane of the second cut. Figure 6a shows that significant stresses are relaxed by the first cut. Figure 6b shows that the remaining stresses, measured by the second cut, are lower magnitude but still very significant. Figure 6c shows the reconstructed original residual stresses. The corresponding stresses measured by neutron diffraction [33], but over the whole cross section instead of half, are presented in Figure 7 for comparison. The root-mean-square difference between the contour and neutron results is 34 MPa for the reconstructed stresses on the second cut, which is only slightly higher than the difference of 28 MPa reported for the first cut stresses [33].

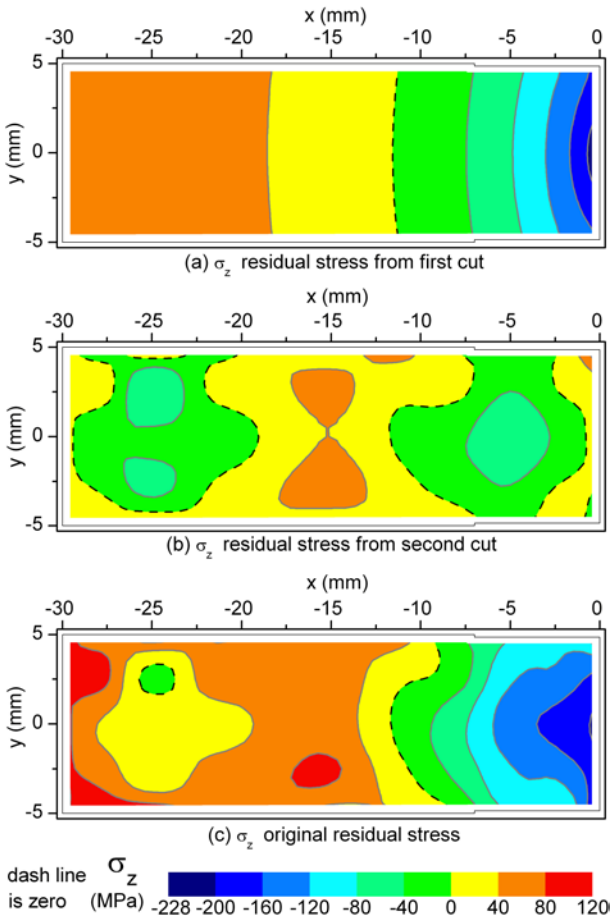

Figure 6. Reconstruction of residual stresses on the second-cut plane. (a) σ_z relaxed by the first cut (**C** in Figure 1), (b) remaining σ_z measured by the second cut (**B**=**E**), and (c) reconstructed original σ_z residual stresses (**A**=**B**+**C**).

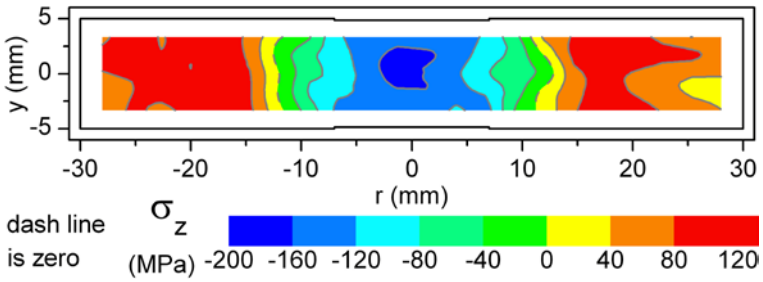

Figure 7. The neutron diffraction map agrees with the contour method stresses (Figure 6c corresponds to half of this map) to a root-mean-square difference of about 34 MPa

Line profiles of stresses are extracted for additional comparison. Figure 8 shows the stresses along the mid-thickness of the disk. Figure 8a shows the reconstruction steps from Figure 6, and Figure 8b shows the comparisons. Considering both experimental and modeling

limitations, the reconstructed stresses are in very good agreement with the neutron diffraction measurements and the FE model of the indentation process [33]. Because the specimen is axisymmetric, the original stresses on the second measurement plane should equal the original stresses on the first measurement plane. Therefore, the stresses measured by the first cut are also plotted. The close agreement between the two contour results indicates both good repeatability of the contour method and also minimal error accumulation from superimposing two contour method measurements for the reconstruction.

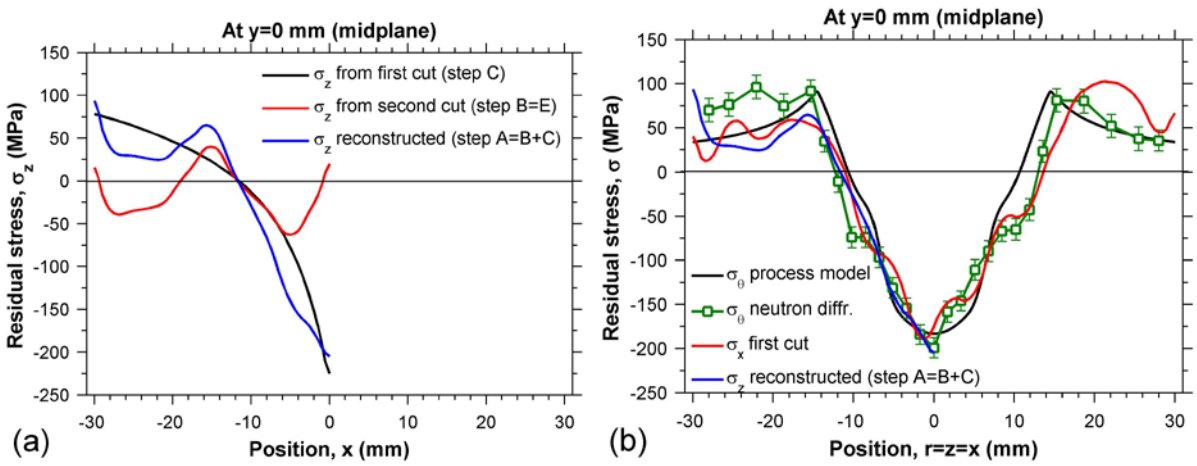

Figure 8. Residual stress profile along disk mid thickness of second cut plane: (a) reconstruction superposition, (b) comparison with FE model of the indentation process [33], neutron diffraction, and contour method results on the first cut (not reconstructed).

Discussion and Conclusions

The ability of the multiple-cut contour method to measure multiple stress components on multiple cross sections is validated using a steel specimen with independently measured residual stresses. The results of contour method and neutron diffraction measurements agree with each other and a finite-element model of the indentation process within 20–35 MPa or 0.010%–0.018% of the elastic modulus.

Compared to the multiaxial contour method, the multiple-cuts method is simpler to implement and does not require an extruded cross section or the assumption that the part is continually processed. The multiaxial method gives stresses throughout a continually processed body as compared on discrete measurement planes. Compared to the surface-superposition contour method, the multiple-cuts method provides the advantage of requiring no additional measurement techniques but the disadvantage of determining different stress components on different cross sections of the part.

The validated superposition principle has much wider application than just contour measurements. Because of experimental limitations, it is common to slice or otherwise reduce the dimensions of a specimen before neutron diffraction [37-42] or synchrotron diffraction [43-46] strain mapping. On occasion, surface stresses are measured using laboratory x-rays on the face of a cut to probe internal stresses [47]. In all these cases, a contour method measurement in conjunction with the cutting steps could address the relaxation issue because the contour method reveals how all stress components have changed throughout the body. Using the contour method and superposition opens up possibilities to combine the advantages of different techniques and obtain unprecedented measurements and understanding.

Acknowledgments

This work was performed at Los Alamos National Laboratory, operated by the Los Alamos National Security, LLC for the National Nuclear Security Administration of the U.S. Department of Energy under contract DE-AC52-06NA25396. Mr. Pagliaro's work was sponsored by a fellowship from the Università degli Studi di Palermo.

References

[1] Withers PJ, Turski M, Edwards L, Bouchard PJ, Buttle DJ (2008) Recent Advances in Residual Stress Measurement. The International Journal of Pressure Vessels and Piping 85:118-127.
[2] DeWald AT, Rankin JE, Hill MR, Lee MJ, Chen HL (2004) Assessment of Tensile Residual Stress Mitigation in Alloy 22 Welds Due to Laser Peening. Journal of Engineering Materials and Technology 126:465-473.
[3] Hatamleh O, Lyons J, Forman R (2007) Laser Peening and Shot Peening Effects on Fatigue Life and Surface Roughness of Friction Stir Welded 7075-T7351 Aluminum. Fatigue and Fracture of Engineering Material and Structures 30:115-130.
[4] Hatamleh O (2008) Effects of Peening on Mechanical Properties in Friction Stir Welded 2195 Aluminum Alloy Joints. Materials Science and Engineering: A 492:168-176.
[5] DeWald AT, Hill MR (2009) Eigenstrain Based Model for Prediction of Laser Peening Residual Stresses in Arbitrary 3D Bodies. Part 2: Model Verification. Journal of Strain Analysis for Engineering Design 44:13-27.
[6] Woo W, Choo H, Prime MB, Feng Z, Clausen B (2008) Microstructure, Texture and Residual Stress in a Friction-Stir-Processed AZ31B Magnesium Alloy. Acta Mat. 56:1701-1711.
[7] Zhang Y, Pratihar S, Fitzpatrick ME, Edwards L (2005) Residual Stress Mapping in Welds Using the Contour Method. Materials Science Forum 490/491:294-299.
[8] Edwards L, Smith M, Turski M, Fitzpatrick M, Bouchard P (2008) Advances in Residual Stress Modeling and Measurement for the Structural Integrity Assessment of Welded Thermal Power Plant. Advanced Materials Research 41-42:391-400.
[9] Kartal M, Turski M, Johnson G, Fitzpatrick ME, Gungor S, Withers PJ, Edwards L (2006) Residual Stress Measurements in Single and Multi-Pass Groove Weld Specimens Using Neutron Diffraction and the Contour Method. Materials Science Forum 524/525:671-676.
[10] Zhang Y, Ganguly S, Edwards L, Fitzpatrick ME (2004) Cross-Sectional Mapping of Residual Stresses in a VPPA Weld Using the Contour Method. Acta Mat. 52:5225-5232.
[11] Thibault D, Bocher P, Thomas M (2009) Residual Stress and Microstructure in Welds of 13%Cr-4%Ni Martensitic Stainless Steel. Journal of Materials Processing Technology 209:2195-2202.
[12] Kelleher J, Prime MB, Buttle D, Mummery PM, Webster PJ, Shackleton J, Withers PJ (2003) The Measurement of Residual Stress in Railway Rails by Diffraction and Other Methods. Journal of Neutron Research 11:187-193.
[13] Evans A, Johnson G, King A, Withers PJ (2007) Characterization of Laser Peening Residual Stresses in Al 7075 by Synchrotron Diffraction and the Contour Method. Journal of Neutron Research 15:147-154.
[14] Martineau RL, Prime MB, Duffey T (2004) Penetration of HSLA-100 Steel with Tungsten Carbide Spheres at Striking Velocities between 0.8 and 2.5 km/s. International Journal of Impact Engineering 30:505-520.
[15] Schajer GS (2001) "Residual Stresses: Measurement by Destructive Testing." Encyclopedia of Materials: Science and Technology, Elsevier, 8152–8158.
[16] Ueda Y, Fukuda K (1989) New Measuring Method of Three-Dimensional Residual Stresses in Long Welded Joints Using Inherent Strains as Parameters-Lz Method. Journal of Engineering Materials and Technology 111:1-8.
[17] Hutchings MT, Withers PJ, Holden TM, Lorentzen T (2005) Introduction to the Characterization of Residual Stress by Neutron Diffraction, Routledge, USA.

[18] Smith DJ, Bouchard PJ, George D (2000) Measurement and Prediction of Residual Stresses in Thick-Section Steel Welds. Journal of Strain Analysis for Engineering Design 35:287-305.
[19] Korsunsky AM, Hills DA (2009) Residual Strain Analysis. The Journal of Strain Analysis for Engineering Design 44:i-iv.
[20] DeWald AT, Hill MR (2009) Eigenstrain Based Model for Prediction of Laser Peening Residual Stresses in Arbitrary 3D Bodies. Part 1: Model Description. Journal of Strain Analysis for Engineering Design 44:1-11.
[21] Korsunsky AM, Regino GM, Nowell D (2007) Variational Eigenstrain Analysis of Residual Stresses in a Welded Plate. International Journal of Solids and Structures 44:4574-4591.
[22] Cheng W (2000) Measurement of the Axial Residual Stresses Using the Initial Strain Approach. Journal of Engineering Materials and Technology 122:135-140.
[23] Smith DJ, Farrahi GH, Zhu WX, McMahon CA (2001) Obtaining Multiaxial Residual Stress Distributions from Limited Measurements. Materials Science & Engineering A A303:281-291.
[24] Beghini M, Bertini L (2004) Residual Stress Measurement and Modeling by the Initial Strain Distribution Method: Part I - Theory. Journal of Testing and Evaluation 32:167-176.
[25] Prime MB, Newborn MA, Balog JA (2003) Quenching and Cold-Work Residual Stresses in Aluminum Hand Forgings: Contour Method Measurement and FEM Prediction. Materials Science Forum 426-432:435-440.
[26] DeWald AT, Hill MR (2006) Multi-Axial Contour Method for Mapping Residual Stresses in Continuously Processed Bodies. Experimental Mechanics 46:473-490.
[27] Kartal ME, Liljedahl CDM, Gungor S, Edwards L, Fitzpatrick ME (2008) Determination of the Profile of the Complete Residual Stress Tensor in a VPPA Weld Using the Multi-Axial Contour Method. Acta Mat. 56:4417-4428.
[28] Pagliaro P, 2008, "Mapping Multiple Residual Stress Components Using the Contour Method and Superposition," Ph.D. Dissertation, Universitá degli Studi di Palermo, Palermo.
[29] Prime MB (2001) Cross-Sectional Mapping of Residual Stresses by Measuring the Surface Contour after a Cut. Journal of Engineering Materials and Technology 123:162-168.
[30] Bueckner HF (1973) "Field Singularities and Related Integral Representations." Mechanics of Fracture G. C. Sih, ed., 239-314.
[31] Pagliaro P, Prime MB, Zuccarello B, 2007, "Inverting Multiple Residual Stress Components from Multiple Cuts with the Contour Method." *Proceedings of the SEM Annual Conference and Exposition on Experimental and Applied Mechanics 2007*, 1993-2005.
[32] Mahmoudi AH, Stefanescu D, Hossain S, Truman CE, Smith DJ, Withers PJ (2006) Measurement and Prediction of the Residual Stress Field Generated by Side-Punching. Journal of Engineering Materials and Technology 128:451-459.
[33] Pagliaro P, Prime MB, Clausen B, Lovato ML, Zuccarello B (2009) Known Residual Stress Specimens Using Opposed Indentation. Journal of Engineering Materials and Technology 131:031002.
[34] Prime MB, Sebring RJ, Edwards JM, Hughes DJ, Webster PJ (2004) Laser Surface-Contouring and Spline Data-Smoothing for Residual Stress Measurement. Experimental Mechanics 44:176-184.
[35] Johnson G, 2008, "Residual Stress Measurements Using the Contour Method," Ph.D. Dissertation, University of Manchester.
[36] Abaqus 6.4, ABAQUS, inc., Pawtucket, RI, USA, 2003.
[37] Brand PC, Prask HJ, Gnaeupel-Herold T, 1997, "Residual Stress Measurements at the NIST Reactor." Physica B, Elsevier, Netherlands, 1244-1245.

[38] Pearce SV, Linton VM, Oliver EC (2008) Residual Stress in a Thick Section High Strength T-Butt Weld. Materials Science & Engineering: A 480:411-418.
[39] Sasaki T, Takahashi S, Kanematsu Y, Satoh Y, Iwafuchi K, Ishida M, Morii Y (2008) Measurement of Residual Stresses in Rails by Neutron Diffraction. Wear 265:1402-1407.
[40] Stacey A, MacGillivary HJ, Webster GA, Webster PJ, Ziebeck KRA (1985) Measurement of Residual Stresses by Neutron Diffraction. Journal of Strain Analysis for Engineering Design 20:93-100.
[41] Stefanescu D, Browne P, Truman CE, Smith DJ (2003) Residual Stress Measurement within a European UIC60 Rail Using Integrated Drilling Techniques. Materials Science Forum 440-441:85-92.
[42] Tawfik D, Kirstein O, Mutton PJ, Wing Kong C (2006) Verification of Residual Stresses in Flash-Butt-Weld Rails Using Neutron Diffraction. Physica B 385-386:894-896.
[43] Buttle DJ, Culham Science Centre A, Collett N, Webster PJ, Hughes DJ, Mills G (2002) A Comparison of Maps and Synchrotron X-Ray Methods: Stresses Measured in Railway Rail Sections. Materials Science Forum 881-886.
[44] de Oliveira U, Ocelik V, De Hosson JTM (2006) Residual Stress Analysis in Co-Based Laser Clad Layers by Laboratory X-Rays and Synchrotron Diffraction Techniques. Surface and Coatings Technology 201:533-542.
[45] Djapic Oosterkamp L, Webster PJ, Browne PA, Vaughan GBM, Withers PJ (2000) Residual Stress Field in a Friction Stir Welded Aluminium Extrusion. Materials Science Forum 678-683.
[46] Webster PJ, Hughes DJ, Mills G, Vaughan GBM (2002) Synchrotron X-Ray Measurements of Residual Stress in a Worn Railway Rail. Materials Science Forum 767-772.
[47] McDonald EJ, Hallam KR, Bell W, Flewitt PEJ (2002) Residual Stresses in a Multi-Pass CrMoV Low Alloy Ferritic Steel Repair Weld. Materials Science and Engineering A 325:454-464.